In vitro experimental investigation of voice production

Stefan Kniesburges, Dipl.-Ing.

Research assistant

Institute of Process Maschinery and Systems Engineering

University Erlangen-Nuremberg

Cauerstr. 4

91058 Erlangen, Germany

Email: kn@ipat.uni-erlangen.de

Phone: +49-9131-8529464

Fax: +49-9131-8529449

Scott L. Thomson, PhD

Associate Professor

Department of Mechanical Engineering

Brigham Young University

435 CTB

Provo, UT 84602, USA

Email: thomson@byu.edu

Phone: +1-801-422-4980

Fax: +1-801-422-0516

Anna Barney, PhD

Senior Lecturer

Institue of Sound and Vibration Research

University of Southampton

Southampton SO17 1BJ , UK

Email: ab3@isvr.soton.ac.uk

Phone: +44-23-8059-3734

Fax: +44-23-8059-3190

Michael Triep, Dipl.-Ing.

Research assistant

Institute for Mechanics and Fluid Dynamics

Technical University Bergakademie Freiberg

Lampadiusstr. 4

09599 Freiberg, Germany

Email: Michael.Triep@imfd.tu-freiberg.de

Phone: +49-3731-39-2362

Fax: +49-3731-39-3455

Petr Šidlof, PhD

Assistant Professor

Institute of Thermomechanics

Academy of Sciences of the Czech Republic

Dolejškova 1402/5

182 00 Praha 8, Czech Republic

Email: sidlof@it.cas.cz

Phone: +420-48535-3015

Fax: +420-28658-4695

Jaromír Horáček, DrSc.

Professor

Institute of Thermomechanics

Academy of Sciences of the Czech Republic

Dolejškova 1402/5

182 00 Praha 8, Czech Republic

Email: jaromirh@it.cas.cz

Phone: +420-26605-3125

Fax: +420-28658-4695

Christoph Brücker, Dr.-Ing.

Professor

Institute for Mechanics and Fluid Dynamics

Technical University Bergakademie Freiberg

Lampadiusstr. 4

09599 Freiberg, Germany

Email: Christoph.Bruecker@imfd.tu-freiberg.de

Phone: +49-3731-39-3833

Fax: +49-3731-39-3455

Stefan Becker, Dr.-Ing.

Assistant Professor

Institute of Process Maschinery and Systems Engineering

University Erlangen-Nuremberg

Cauerstr. 4

91058 Erlangen, Germany

Email: sb@ipat.uni-erlangen.de

Phone: +49-9131-85-29455

Fax: +49-9131-85-29449

January 20, 2011

Abstract

The process of human phonation involves a complex interaction between the physical domains of structural dynamics, fluid flow, and acoustic sound production and radiation. Given the high degree of nonlinearity of these processes, even small anatomical or physiological disturbances can significantly affect the voice signal. In the worst cases, patients can lose their voice and hence the normal mode of speech communication. To improve medical therapies and surgical techniques it is very important to understand better the physics of the human phonation process. Due to the limited experimental access to the human larynx, alternative strategies, including artificial vocal folds, have been developed. The following review gives an overview of experimental investigations of artificial vocal folds within the last 30 years. The models are sorted into three groups: static models, externally driven models, and self-oscillating models. The focus is on the different models of the human vocal folds and on the ways in which they have been applied.

Keywords: artificial vocal folds, flow-induced acoustics, fluid-structure-acoustic interaction, glottal fluid flow, human phonation, structural dynamics, voice

Abbreviations:

- PIV: Particle image velocimetry
- FOT: Forced oscillation technique
- M5: One specific vocal fold model geometric definition
- MRI: Magnetic resonance imaging
- Re: Reynolds number
- St: Strouhal number

1 Introduction

The human voice is the result of the physical process known as phonation. The basic tone of the voice originates from the oscillating vocal folds inside of the human larynx, which is situated in the neck (see fig. 1). The normal voice can be explained by the linear source-filter principle with the vibrating vocal folds as the acoustic source and the oral and nasal open cavity-resonator as a filter [1, 2, 3, 4, 5] (see fig. 1). The physical process can be characterized therefore by a fluid-structure-acoustic interaction.

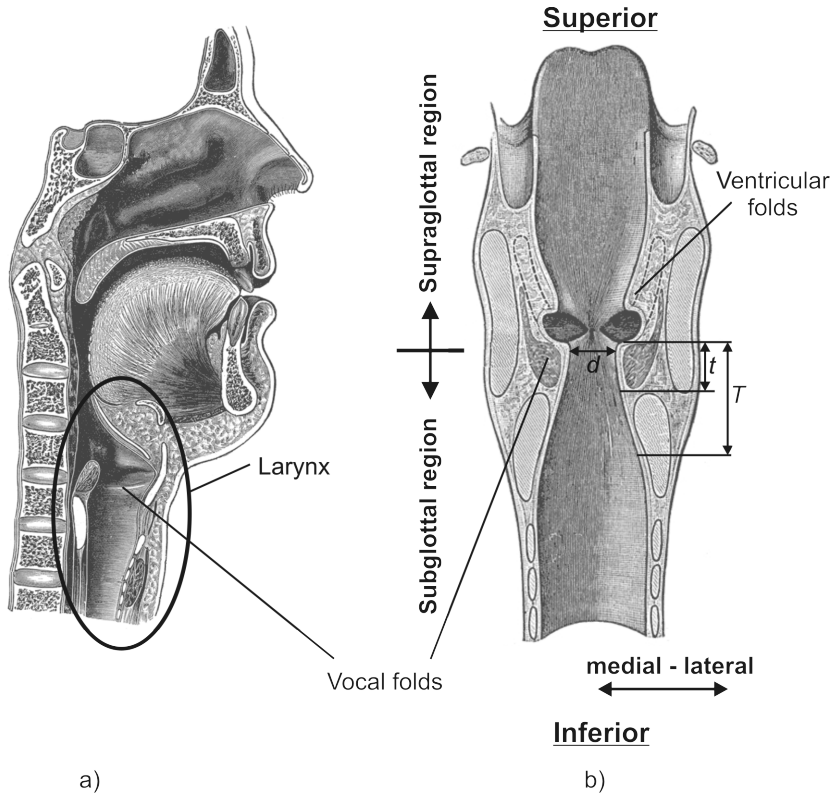

Figure 1: Schematic of the human larynx based on Gray [6]: a) Sagittal cross-section of the human head and neck, with the position of larynx within the neck denoted. b) Coronal cross-section of the human larynx along with the following geometrical parameters: diameter of the glottis d, thickness of the vocal folds T, and the length of the glottal duct t.

A variety of dysfunctions in this complex process have been observed that can

drastically influence human phonation. In most cases asymmetric vibration patterns of the vocal folds are responsible for these dysfunctions [7], causing hoarseness, or – in the worst case – a total loss of voice. For medical treatment several diagnostic techniques have been developed, such as electroglottography [8], stroboscopy [9] and high-speed endoscopy [10], which are mainly used to investigate the structural dynamics during phonation. For a detailed understanding of the fully-coupled physics, flow and acoustic contributions also have to be considered. It is almost impossible to measure flow field characteristics, including pressure distributions, in sub- and supraglottal regions in vivo. While excised human or animal larynges offer better access to all regions, the availability of test subjects is very restricted. Furthermore, it is difficult to reproduce basic conditions comparable to the living state.

To overcome the limitations of in vivo test conditions, studies using artificial experimental larynges began many years ago. In 1957 van den Berg [11] published a study of a static model of the vocal tract in which he investigated flow resistance and the Bernoulli effect within the glottal duct. Since then, numerous experimental strategies have been developed for vocal tract modeling. The models can be classified into three main groups. First are static models with fixed, rigid walls and mostly up-scaled geometrical dimensions to allow higher spatial resolution of the flow field. The main focus of static model experiments lies in aerodynamic studies because detailed measurements of the flow within the glottis with fixed boundary conditions can be performed. Using similarity principles the aerodynamic time scales are longer in up-scaled models and can be transferred back to life-size dimensions. Second, in the last decade of the 20th century the motion of vocal fold models was incorporated by externally driving the periodic movement of the model glottal walls. Scaling up the geometrical dimensions – and in a few cases changing the operating fluid to water – enabled detailed studies of how the flow field depends on the motion of the vocal fold models. With new optical measurement techniques in fluid dynamics, fundamental flow phenomena could be explored in supraglottal regions. Third, in the past 10 to 15 years structural deformation has also been taken into consideration in the experimental strategies in order to study full fluid-structure interaction dynamics. Synthetic models of the vocal folds – mostly of human

length-scale – were developed using materials with similar characteristics to vocal fold tissue that exhibited life-like behaviour. They predominantly consisted of polyurethane or silicone rubber, whose elasticity could be varied down to the very low Young's moduli that is characteristic of vocal fold tissue (on the order of a few kPa) [1]. With these models it became possible to produce self-sustained, flow-induced vibrations at characteristic frequencies that compared to those found in the human vocal folds. Consequently, in addition to aerodynamic studies, acoustic production and structural motion could be analyzed and compared to in-vivo measurements of human phonation.

The current paper summarizes studies reported by international groups in the field of experimental modeling of human phonation from the last 30 years. The three different groups of models are described in the order of the experimental strategy:

- **Static models:** Rigid, fixed vocal fold models
- **Driven models:** Moving, externally-driven vocal fold models
- **Fully-coupled models:** Self-oscillating vocal fold models consisting of elastic material with characteristic material properties

2 Physics of the human phonation process

2.1 Anatomy of the human larynx

The human larynx is located below the oral cavity and above the trachea that connects to the bronchial tube leading to the lungs. It consists of both hard and soft tissues. The hard tissues that surround the flow region include four cartilage structures: the thyroid, cricoid, arytenoid, and epiglottis cartilages, as displayed in fig. 2. The only bone in the larynx, the hyoid bone, is a horseshoe-shaped structure that spans the entry to the larynx.

Within this hard framework are soft tissues, including the vocal folds and the ventricular folds (fig. 1). The **V**-shaped gap between the two vocal folds (see fig. 3) is called the glottis. During normal breathing the glottal gap is open to

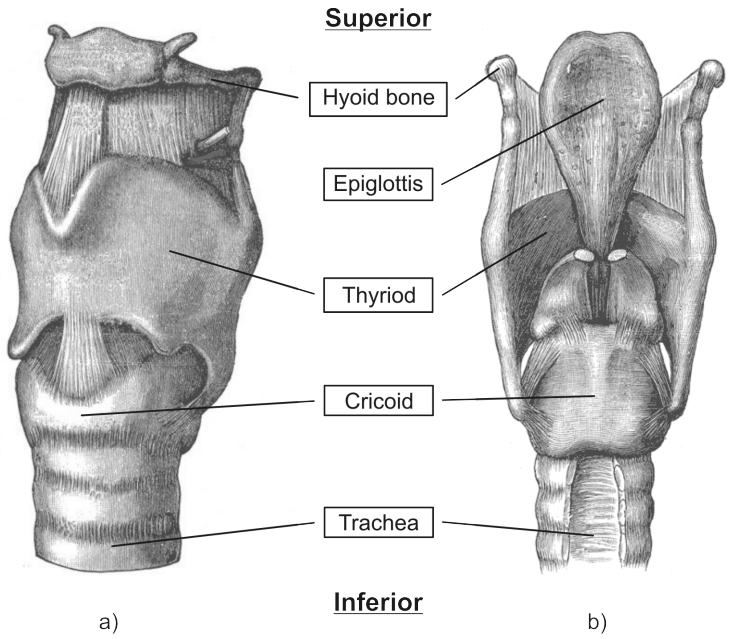

Figure 2: Schematic of the human larynx framework, based on Gray [6]: a) Posterior view (front). b) Anterior view (back).

allow for air exchange. For speaking, the glottis is closed and the air stream arising from the lungs excites the vocal folds to vibration, producing the basic tone of the human voice.

The inner morphology of the human vocal folds is composed of multiple layers of tissue (fig. 4). The epithelium is the outermost layer and covers the soft lamina propria, which is further divided into superficial, intermediate, and deep layers. Whereas the fluid-like superficial lamina propria consists of a loose compound of statistically stationary oriented elastin fibers mixed with interstitial fluids, the intermediate and deep lamina propria layers are composed of elastin and collagen fibers which are oriented longitudinally to the vocal folds. Therefore the lamina propria is thought to define the elasticity of the vibratory portion of the vocal folds. The thyroarytenoid muscle can also be further structured into two bundles: the thyrovocalis which is responsible for the fine-tuning of the tension within the fibers of the lamina propria and the thyromuscularis for a quick shortening of the vocal folds. These tissue layers are commonly grouped as follows: the cover (epithelium and superficial lamina propria), the

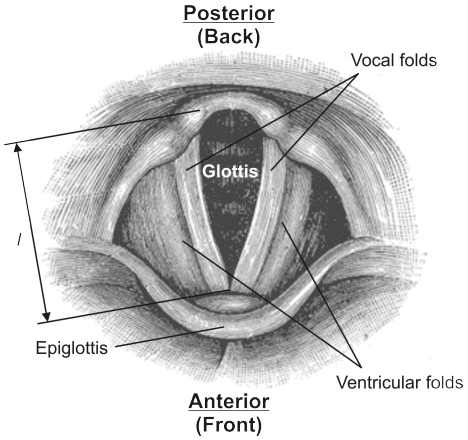

Figure 3: Schematic of the top view of the human larynx, based on Gray [6] along with the following geometrical parameter: anterior-posterior length of the vocal folds l.

ligament (intermediate and deep layers of the lamina propria), and the body (thyroarytenoid muscle) [1].

In normal speech the ventricular folds (fig. 1) do not oscillate, and therefore do not apparently contribute directly or significantly to the acoustical production. Aerodynamically, they constitute a divergent constriction downstream of the glottis which reduces the pressure drop across the glottal constriction. However their function is still the focus of current research [12, 13, 14, 15].

Besides the production of the human voice, it is here briefly noted that the larynx performs the important function of protecting the lower respiratory system from infiltration of such foreign objects as liquids or solid bodies. This is done by closing the laryngeal duct by the epiglottis, mainly during the swallowing process. As this function is not the subject of this article, it is not discussed further here.

2.2 Voice production dynamics

The vocal folds are excited by an airstream from the lungs and undergo large-amplitude oscillations. These oscillations form a pulsatile supraglottal jet, the associated pressure fluctuations of which constitute the primary acoustic source

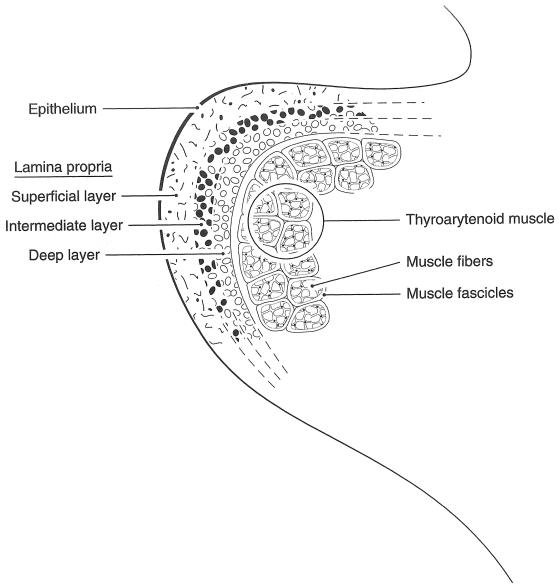

Figure 4: Inner morphology of the vocal fold, based on Titze [1]: Within the intermediate layer the empty dots mark the elastin fibers, whereas the black-filled dots in the deep layer denote the collagen fibers.

for human phonation. This acoustic source is filtered by the upper vocal tract, thereby forming the final voice signal which radiates from the mouth into the ambient air. Due to the flow-driven oscillations of the vocal folds, and the resulting acoustic production, phonation can be described as a fluid-structure-acoustic interaction process. Air passes over the elastic tissues of opposing vocal folds, which are deformed by the fluid forces. This deformation constitutes a change in the fluid flow boundary conditions. During this dynamic process the acoustic production of the basic tone occurs.

Due to the multi-layer structure of the vocal folds, the geometry of the glottal duct changes during a vibration cycle from a convergent to a divergent shape, as displayed in fig. 5. This particular periodic motion is described as a mucosal wave [16] (since the cover layer of the vocal folds is often referred to as the vocal fold mucosa). During this motion the epithelium and lamina propria layers move relative to the nearly stationary thyroarytenoid muscle (the vocal fold body).

The oscillations are sustained by the periodic exchange of energy between air flow and vocal fold elastic tissue dynamics. During normal speech the acoustic

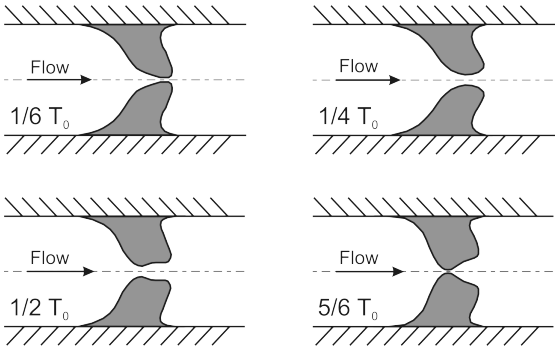

Figure 5: Schematic of the geometry of the glottal duct during oscillation at four different instances of a glottal period T_0 [19].

coupling between the fluid flow and the structural dynamics is negligible and the phonation process can be described by the linear source-filter model. However, in professional male-singing at very high pitches, for example, a harmonic-formant interaction can occur, enhancing vocal fold oscillations and leading to a change in oscillation patterns [17, 18].

2.3 Physical parameters

The phonation process is often characterized by a few key physical parameters. These parameters generally correspond to the different physical domains. Table 1 summarizes some of the most important fluid, tissue, and geometric parameters. It is important to note that these values may only be considered as representative, since there are large variations in different laryngeal tissues due to factors such as individual subject health, gender, age, genetics, and different voicing conditions. Furthermore, parameters such as onset pressure or vocal fold elasticity can often only be determined in experiments using excised larynges. In many cases parameters used in numerical or experimental models originates from excised canine larynges due to their availability and their similarity to human larynges.

For more detailed information about the overall phonation process, including geometry as well as fluid and structural dynamics, readers are referred to works such as Titze [1, 2], McCoy [5] and Thomson [20], and references found therein.

For more details of the structural properties of the vocal folds, see, for example, Min et al. [21], Tran et al. [22] and Chan and Rodriguez [23].

Table 1: Physical parameters of the human phonation process

Vocal fold length (anterior-posterior)	$l = 10 - 17\,\mathrm{mm}$
Vocal fold thickness (inferior-superior)	$T = 9 - 10\,\mathrm{mm}$
Glottal gap diameter	$d = 0 - 5\,\mathrm{mm}$
Glottal duct length	$t = 2 - 5\,\mathrm{mm}$
Subglottal oscillation threshold pressure	$P_{th} = 200 - 1000\,\mathrm{Pa}$
Maximum intraglottal velocity	$U_{\max} = 10 - 40\,\mathrm{m/s}$
Fundamental frequency	$f = 80 - 300\,\mathrm{Hz}$
Reynolds number	$Re = \frac{U_{\max} w_{\mathrm{G,max}}}{\nu} = O(10^3)$
Mach number	$Ma = \frac{U_{\max}}{c} = O(10^{-1})$
Strouhal number	$St = \frac{f\, w_{\mathrm{G,max}}}{U_{\max}} = O(10^{-2})$
Average vocal fold Young's modulus	$E = 5 - 20\,\mathrm{kPa}$

3 Static models

Static models have a long history in laryngeal modeling, with one of the earliest recorded studies being a brass replica of the trachea and vocal folds reported by Wegel [24] in 1929. The first in a line of more recent static modeling experiments was conducted by van den Berg [11] in 1957 using a plaster cast of an excised canine larynx. Since that time static models have been used to investigate the translaryngeal pressure drop, intraglottal pressure and flow profiles, supraglottal jet formation, the transition of the glottal flow to turbulence, flow symmetry, and broadband sound generation, all in a variety of flow-channel geometries that mimic those found at different stages of the glottal cycle during phonation. Over this period, the so-called "M5" model geometry, first proposed by Scherer et al. [25], has been widely adopted as the benchmark static larynx geometry (see fig. 6) and, as reported by Pickup and Thomson [26], has been adapted for use in studying acoustically and aerodynamically-driven vibration modes [27], characterizing vortex development downstream of the glottis [28],

developing devices for measuring in vivo flow properties [29], estimating the material response of the vocal folds [30] and the strength of fluid-structure and acoustic-structure interactions [31], and considering the acoustical influence of mammalian air sacs on voice quality [32].

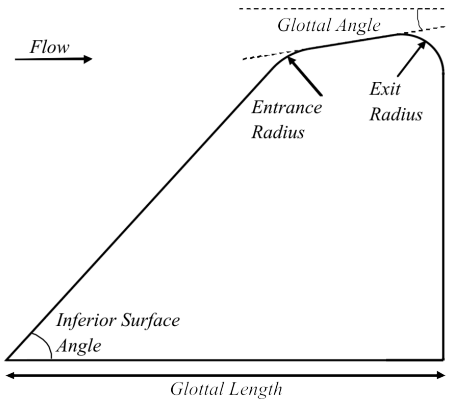

Figure 6: Schematic of the M5 vocal fold model. For appropriate dimensions and geometric constraints, see Scherer et al. [12]

The use of static models to investigate the flow in and around the glottis is predicated on the assumption, commonly made in theoretical larynx modeling (e.g. [33]), that the flow through the glottis is quasi-steady. That is to say, the pressure and flow distributions due to a given translaryngeal pressure drop in a flow channel of fixed geometry may be considered to be the same as would be found at a particular moment in the vibrating larynx, for the same translaryngeal pressure drop, when the geometry was instantaneously identical to that of the fixed channel. Thus fixed geometry models may be considered to provide a "snap-shot" of the instantaneous pressure and flow conditions at a given moment of the glottal cycle.

The shape of the human larynx varies with distance along all three of its principal axes. In modeling studies, however, it has been customary to consider variation in only two dimensions and to choose a rectangular cross-sectional area for the glottal slit. This is the case for all studies considered here except where explicitly stated otherwise. A conventional of calling the extent of the glottis in the direction parallel to the flow the thickness, t, typically of the order of 0.4 cm in men and 0.25 cm in women, the glottal distance from the arytenoid

cartilage to the thyroid cartilage the length, l, typically 1.0 to 1.7 cm and the dimension that varies as the vocal fold vibrate the glottal gap diameter, d, typically 0 to 0.5 cm is adopted throughout this section regardless of the naming convention used by the authors of each paper discussed.

3.1 Aerodynamics

The most common use of static models is to investigate glottal aerodynamics. A prescribed volume flow is drawn through a shaped channel, and pressure at the channel wall is measured at one or more locations using manometers or other pressure transducers connected to small tap holes drilled in the model. When the predominant interest is in the flow and pressure profiles, static models may be constructed with geometries several times bigger than life-size, provided that the Reynolds number (Re) based on the glottal diameter is kept within the realistic range (up to approximately $Re = 3000$ for typical glottal diameters and flow rates) for phonation by also scaling the volume flow rate either directly or by scaling the driving pressure.

The vibration of the vocal folds is driven by the transglottal pressure drop. An early study by Scherer et al. [34] investigated the variation of volume flow rate through a life-size glottal model as the transglottal pressure was varied from 300 to 1600 Pa (3 − 16 cmH_2O). Two geometries were considered for the glottal channel, both with rectangular glottal profiles: model M1 had dimensions typical for an adult male with a minimum glottal diameter, d, of 0.104 cm with an anterior-posterior length, l, of 1.2 cm, and a glottal thickness, t, of 0.37 cm; model M2 was somewhat larger having minimum glottal diameter, d, of 0.158 cm, with an anterior-posterior length, l, of 2.019 cm and a glottal thickness, t, of 0.625 cm. Comparison of the measured transglottal pressure drop for a given volume flow rate with the theoretical model of Ishizaka and Matsudaira's turbulent equation [33] found agreement to within ±10% for both models although agreement was better for the smaller model M1. Agreement with the theoretical formulations of Wegel [24] and van den Berg et al. [11] was less close.

In 2006 Fulcher et al. [35] returned to the question of the variation of trans-

glottal pressure with volume flow rate using the M5 model and considering a wide range of different glottal geometries (transglottal pressures of 3, 5, 10 and 15 cmH_2O; minimum glottal diameters of 0.005, 0.02, 0.02, 0.08, 0.16 and 0.32 cm; glottal angles of 40°, 20°, 10°, 5° convergent and divergent and a uniform glottis) and deriving a generalized equation to predict flow from the pressure drop and geometric information. They reported that this generalized formulation predicted volume flow rate more accurately than either the equations of Ishizaka and Matsudaira [33] or the equation of van den Berg et al. [11].

A large number of studies have used static models to investigate the variation of pressure profile along the glottal axis parallel to the mean flow. The earliest study was that of van den Berg et al. [11] which used a life-sized model with a rectangular glottis of length $l = 1.8$ cm, thickness $t = 0.32$ cm and a diameter that could be varied from $d = 0.01$ to 0.32 cm. Subglottal pressure ranging from 0 to 64 cmH_2O resulted in volume flow rates of up to 2 l/s. The pressure downstream of the glottis was assumed to be atmospheric. Defining the glottal resistance R as the ratio of the subglottal pressure to the volume flow rate they found that at small volume flow rates and/or glottal diameters the resistance was dominated by friction effects with

$$R = \frac{12\mu t}{ld^3} \tag{1}$$

where μ is the dynamic viscosity of the air, but at large volume flow rates and or large glottal diameters turbulence was dominant with

$$R = \frac{12\mu t}{ld^3} + 0.875\frac{\rho U}{2l^2d^2} \tag{2}$$

where U and ρ are the volume flow rate and density of the air respectively. Defining the kinetic pressure in the glottis as $P_{\text{kin}} = \frac{1}{2}\rho v^2$, where v is the velocity on the glottal axis, van den Berg et al. found that the pressure loss at the glottal inlet, the entry loss, was approximately equal to $(k_1 \cdot P_{\text{kin}})$ where $k_1 = 1.37$ and the pressure recovery at the glottal exit, the exit recovery, was approximately equal to $(k_2 \cdot P_{\text{kin}})$ where $k_2 = -0.5$ independent of the transglottal pressure.

Binh and Gaufin [36] also explored the intraglottal pressure distribution using a model that was 5 times life-size and had two stacked sections to its vocal folds so that, by protruding one or other to a greater or lesser degree, the glottal channel could be converging, diverging or parallel-sided. The model was supplied with a constant volume flow in the range 0 to 1500 cm^3/s. Calculation of the entry loss and exit recovery coefficients showed them to vary in a complex way with the glottal geometry and the Reynolds number. In the Reynolds number range found in phonation (given as $\sim 200 - 800$) the entry loss coefficient ranged from $k_1 = 1.4$ to 1.8 and the exit loss coefficient from $k_2 = -0.05$ to -0.17, suggesting that the value of -0.5 found by van den Berg et al. was too high and would consequently underestimate the transglottal pressure drop. Binh and Gaufin's measurements also revealed that the forces on the lower vocal fold edge could be very large and that positive pressures were found in this region for small openings with laminar flow, but that negative pressures could develop there when the glottal channel was diverging. Forces on the upper parts of the folds were found to be relatively much smaller.

Scherer et al. [25] considered the effect of varying the radius of curvature of the glottal exit on the glottal flow resistance and the intraglottal forces in a converging larynx model for a volume flow rate of 73.2 cm^3/s and a minimum glottal diameter of 0.02 cm. They found that transglottal and intraglottal pressures increased, thus increasing flow resistance and force on the vocal folds as the exit radius of curvature decreased.

Li et al. [37] looked at the variation of intraglottal pressure in a model with a glottis having glottal angles of 2.5°, 5°, 10° and 20° for both convergent and divergent channels, and also a uniform channel. The minimum glottal diameter was 0.06 cm, the model was 1.7 times life-size and volume flow rate ranged from 0 to 500 cm^3/s. They found that greater convergent glottal angles resulted in greater outward driving forces acting on the vocal folds and that glottal flow resistance was greatest for the uniform glottis and least when the glottis was divergent with an angle of 10°. Further, they observed that the greatest negative pressure in the glottis occurred for a diverging channel with an angle of 10°, associated with the greatest pressure recovery, and that the smaller the convergent glottal angle the greater the flow resistance. They suggested that

phonatory efficiency may be enhanced if there are large convergent angles during glottal opening and small divergent angles during closing.

In an extension to the well-documented M5 geometry, Scherer et al. have recently published data on model M6 which has a glottal channel with a realistic geometry in three dimensions [38]. Like M5, this model is 7.5 times life-size and can be configured to have a glottis with 10° convergent, parallel, or 10° divergent profile in the flow direction. Additionally, however, this model has a concave profile along the length of the vocal folds in the direction perpendicular to the flow which gives an elliptical shape to each plane of the glottal channel. Three sets of fourteen pressure taps were drilled in a line across the vocal fold surface: one set was parallel to the plane just inside the entrance; one was mid-way along the glottal channel, and one was just upstream of the exit plane. The sets of taps were designed to allow exploration of the pressure variation across each plane at different points along the glottal axis. Little difference was found between the different pressure taps for the set near the entrance, but small pressure gradients were measured between the members of the middle set and between the members of the set at the glottal exit, suggesting slight variation from the one-dimensional model frequently assumed in theoretical formulations of the glottal flow.

Two studies have looked at the intraglottal pressure profile specifically in hemilarynx models in order to make comparisons with hemilarynx data obtained from excised larynx experiments. In a hemilarynx model the glottal channel is asymmetric, with one wall following a typical vocal fold shape while the other is a plane surface. Alipour and Scherer [39] measured whether pressure taps on the plane surface gave identical pressure measurements to taps on the shaped wall at equivalent positions and found that the pressure measured on the plane wall was systematically lower than that measured on the shaped wall for all locations at all glottal diameters (range $d = 0.04$ to $0.25\,\mathrm{cm}$) and transglottal pressure drops (8, 16 and $34\,\mathrm{cmH_2O}$) considered. The downstream pressure recovery was greater than for symmetric larynx models which they ascribed to the effect of a less abrupt channel expansion at the glottal exit. Fulcher et al. [40] also considered the hemilarynx for a minimum glottal diameter of $0.04\,\mathrm{cm}$ with transglottal pressure drops of 3, 5, 10, 20 and $40\,\mathrm{cmH_2O}$ with one plane

wall to the glottal channel and one with a more realistic vocal fold shape with either a convergent channel of 5°, 10° or 20°, a parallel profile or a divergent channel with an angle of 5°, 10° or 20°. The pressure distribution was found to be bistable (except for the 20° convergent case) with a glottal jet skewed to the left or the right side of the pharynx even when the glottal channel had two parallel walls. The pressure difference between the plane and shaped walls was of the order of $7-8\%$ for the 10° divergent channel and closer to 12% for the 20° divergence. Intraglottal pressures for this hemilarynx configuration were of the same order of magnitude as found in symmetric larynx models.

Although the existence of flow asymmetry in asymmetric channels such as the hemilarynx might be expected, the question of whether the flow is also skewed in symmetric glottal channels has been studied in some detail by a number of researchers. A tendency of flow to attach preferentially to one wall of a channel can arise when the entrainment of fluid by a jet is limited by the presence of the channel boundary, causing the jet to skew towards the wall. This is known as the Coanda effect [41]. The term Coanda effect is sometimes also used more loosely by the laryngeal modeling community to describe any skewing of a jet flow whether caused by the presence of a channel boundary or by, for example, the jet entering a region of already disturbed flow.

Pelorson et al. [42] considered jet skewing in a simple, fixed geometry model of the glottis that was three times life-size. The model had symmetrical, hemispherical constrictions, each with a radius of curvature of 1 cm, representing the vocal folds with a minimum glottal diameter ranging between 0.01 and 1 cm. With a steady flow through the channel, the pressure on each side of the constriction, measured where the diameter was minimum, showed a difference that suggested the flow between the vocal folds exhibited a skewing effect. However, they also considered the case when the flow was impulsively started by means of a blade valve upstream of the glottis such that the flow between the folds was unsteady. Under these conditions the pressure at the minimum glottal diameter was the same on each side suggesting, that the unsteady jet remained symmetric.

Scherer et al. [12] considered the Coanda effect in model M5 with a symmetric,

divergent glottis having an angle of 10° and also with an asymmetric glottis that diverged with an angle of 10° and was additionally angled obliquely at 15°. The minimum glottal diameter was 0.04 cm in both cases. Differences in the intraglottal pressures suggested that there was flow asymmetry in the symmetric as well as the asymmetric flow channel except at the very lowest transglottal pressure considered (3 cmH_2O). In the symmetric case the pressures on the two walls differed by 5 to 6% of the transglottal pressure and in the oblique case by as much as 27% of the transglottal pressure. Shinwari et al. [43] replicated these pressure distribution results. A further study in 2002 [44] considered a symmetric glottal channel and one with an oblique angle of 20°, both with parallel channel walls, finding that pressures measured on the two sides of the channel remained equal, except right at the glottal exit for the symmetric channel, but differed by 21.4% of the transglottal pressure for the oblique channel.

Hofmans et al. [45], building on the work of [42], considered pulsatile flow in a rigid glottal channel replica and proposed that an asymmetric flow took a time to develop that was longer than a typical glottal period and hence that the Coanda effect was unlikely to occur during human phonation.

Erath and Plesniak [46] considered pulsatile flow in a 7.5 times life-size, fixed-geometry glottis with divergence of 10°, 20° and 40°. Both Reynolds number and Strouhal number St were scaled to give values equivalent to $Re = 0$ to 2000 and St corresponding to fundamental frequencies of 100 to 150 Hz. For the divergent glottis the separated flow was skewed in both the 10° and 20° cases and re-attached to one of the channel walls, but in the 40° case there was no re-attachment to the walls after the initial separation. They suggested that the Coanda effect may be a function of flow acceleration rather than an effect based on absolute temporal scale and pointed out that the measurements of [42] and [45] were not in contradiction with this view.

Park and Mongeau [47] considered the applicability of the quasi-static approximation in glottal models using both static and dynamic, self-oscillating rubber glottal models. They determined that the quasi-static approximation was valid for around 70% of the glottal duty cycle for a fundamental frequency of 100 Hz

and Reynolds numbers, based on the square root of the glottal area, of greater than 3000. It was not valid at lower Reynolds numbers however, when the influence of viscosity and the effects of the motion of the glottal walls were large, mainly at the beginning and end of each cycle when the glottis was narrow.

Early models (e.g. [11], [36]) had a supralaryngeal geometry that incorporated a widening of the vocal tract, corresponding to the laryngeal ventricle, and a contraction above this that mimicked the shape of the ventricular folds. These authors made no specific attempt, however, to characterize the effects of the ventricular folds on the glottal resistance. The effect of these anatomical, was first systematically investigated by Bailly et al. [13] who used a rigid model as one aspect of their study. The ventricular folds were included as an additional, rigid constriction in the flow channel. They measured the pressure upstream of the glottis, in the laryngeal ventricle, and at the point of minimum diameter on both sides of the ventricular glottis. Both the glottal diameter and the diameter of the ventricular glottis were variable, with the glottal diameter ranging from 0 to 0.595 cm and the ventricular glottal diameter from 0.004 to 2.6 cm. For translaryngeal pressures ranging from 0 to 100 Pa, they found that the pressure in the ventricular glottis was negative and the pressure distribution there was asymmetric and bistable, although the asymmetry took time to become established. When the translaryngeal pressure reached 500 Pa the pressure distribution throughout the glottal channel depended significantly on the ratio of the minimum glottal diameter to the minimum diameter of the ventricular glottis with small ventricular glottis diameters tending to reduce the pressure asymmetry. Li et al. [48] also used a static model to investigate the effect of the ventricular folds on the intraglottal pressure. They considered twelve ventricular glottis diameters from 0.02 to 2.06 cm for each of a 40° convergent, uniform, and 40° divergent true glottis with a minimum diameter of either 0.04 or 0.06 cm and a transglottal pressure of 8 cmH_2O. Intraglottal pressures were lowest and flow rate highest for ventricular glottis diameters of 1.2 to 2 times the minimum glottal diameter. The divergent glottis gave lower intraglottal pressure and higher flow than the convergent and uniform cases and the ventricular vocal folds decreased the effects of the glottal angle. The ventricular folds also moved the flow separation point downstream in the true glottis, straightened

the glottal jet, decreased laryngeal resistance, and reduced energy dissipation.

Some studies that considered the intraglottal pressure profile also made direct measurements of the glottal flow and yet others considered the flow exclusively. Binh and Gaufin [36] explored the glottal flow pattern through visualisation using the Schlieren technique. A jet, separating from the walls of the glottis and emerging into the laryngeal ventricle, was observed. Pelorson et al. [42] also observed a separated jet with the characteristic rolling up of the shear layer into ordered vortical structures when they seeded the impulsive flow through their model with smoke particles. Alipour et al. [49] use a hotwire anemometer to measure the velocity upstream and downstream of their model glottis. Upstream of the glottis they observed parabolic, laminar flow profiles, but on the downstream side the flow was turbulent and developed asymmetric profiles when the glottis had a divergent shape. For a minimum glottal diameter of 0.06 cm and Reynolds numbers in the range 1000 to 2000 they observed that as the Reynolds number increased the upstream parabolic velocity profiles flattened, consistent with the expected shape for a flow that is not fully developed. The observed patterns corresponded well to their observations in excised larynges and to the predictions of a computational model.

Shinwari et al. [43] visualized the flow in the M5 model and observed a separated flow, where the separation point remained constant as the flow speed increased for a uniform glottis, but moved upstream with increasing flow rate in the oblique glottis case. In all geometries they observed skewing of the jet and flow recirculation regions downstream of the glottis. The laminar core of the jet had a length of the order of 0.6 cm, decreasing as the flow speed increased.

In a rigid model with a transient flow, Hofmans et al. [45] investigated the transition to turbulence in the glottal jet. They found that, like the Coanda effect, the transition to turbulence takes time to establish and may not therefore occur during a normal phonatory cycle. Erath and Plesniak [46] considered pulsatile flow in a rigid divergent glottal model and used particle image velocimetry (PIV) to observe that for glottal angles of 10° and 20° the flow was bistable, eventually attaching to one or other of the glottal walls, while for a glottal angle of 40°, the flow did not attach to either wall.

In a divergent model with a minimum glottal diameter of 0.04 cm which had the option to incorporate ventricular folds, Kucinschi et al. [50] found a glottal jet with a laminar core and a turbulent mixing region with ordered vortex shedding. The presence of the ventricular folds lengthened the flow structures and reduced the jet curvature and, when the ventricular glottis was narrow, delayed the vortex shedding. The speed of vortex transport downstream of the glottal exit was found to be of the order of 0.3 to 0.4 times the jet centreline velocity, which is slightly lower than the value of 0.5 times the jet velocity widely reported for free jets emerging from sharp edged orifices.

3.2 Aeroacoustics

Studies using static models to investigate sound production are sparse for the obvious reason that the primary source of sound during phonation comes from the dynamic action of the laryngeal vibration. Zhang et al. [51] used a fixed glottal channel to consider the broadband noise generation due to the glottal jet. They used relatively rigid rubber vocal fold models with a number of different glottal profiles, each representing one possible channel shape that could be found during a glottal cycle. They measured the radiated sound spectra for a variety of flow speeds, channel shapes, and gas mixtures, and extracted from them an estimate of the acoustic source function. They found that for circular jets in parallel and converging glottal channels, quadrupole-like sound sources were the dominant acoustic mechanism, and that for a diverging glottis, whistle tones occurred at low flow speeds with dipole-like behaviour dominant at high flows. They observed, however, that acoustic feedback effects may have adversely influenced the source identification technique. Kucinschi et al. [50] measured an acoustic signal in model M5 with a divergent glottal channel and ventricular folds. The acoustic signal was very weak for normal speech flow rates ($22 - 222\,\mathrm{cm}^3/\mathrm{s}$) but stronger for flow rates found in loud speech ($444 - 667\,\mathrm{cm}^3/\mathrm{s}$). At the higher flow rates they suggest that both dipole and quadrupole sources might be present when the diameter of the ventricular glottis was small, but that only quadrupole sources were active for larger ventricular glottis diameters.

3.3 Other study focuses

One study by Cisonni et al. [52] makes a somewhat different use of a static mechanical model. Usually in theoretical modeling the transglottal pressure drop is estimated from the subglottal pressure and the glottal geometry. In this study theoretical flow models were inverted to estimate the subglottal pressure, the minimum glottal diameter, or the flow separation coefficient. Measurements made on a static model were used to test the realism of the predictions of the inverse models, and it was found that, providing viscous effects are adequately incorporated into the formulation, the inverse models perform well as predictors of these various glottal parameters.

4 Externally-driven models

In the following sections we describe two different types of driven models. The first type of model is one in which the entire model is moved uniformly in a rigid-body translational sense; thus, the model motion is in phase with itself. In these cases the direction of motion is strictly medial-lateral. The second type is one in which the model moves such that there is a phase difference in the lateral motion of different regions of the model. In these cases some of the models contain slight inferior-superior as well as medial-lateral motion (see fig. 1). These models have been used for a variety of purposes, such as to characterize glottal flow, evaluate analytical and theoretical models, and provide data for computer code validation. In the following sections we include both the model descriptions and their stated uses.

4.1 Uniform-phase driven models

Synthetic, driven vocal fold models have been utilized to determine whether the flow through the vocal folds may be approximated as being quasi-steady, or whether it is inherently unsteady. Krane et al. [53] described tests on a scaled-up facility for approximating the flow through the human vocal folds. The model consisted of symmetric half-cylindrical shapes mounted within an

open-ended duct that was submerged in an open water channel. The model scale was 10 times that of the human vocal folds, with an inferior-superior glottal dimension of 12.7 cm. The model was constructed of clear, rigid acrylic. Medial-lateral displacement was controlled via stepper motors and linear stages. Matching Reynolds and Strouhal numbers for the human vocal folds yielded a model period of 15 s. Particle image velocimetry was used to obtain glottal and supraglottal jet velocity fields along the coronal plane. The PIV sampling frequency was 15 frames per second (fps), which, when combined with the 15 s oscillation period, allowed for real-time sequential PIV image acquisition. Observations of velocity data suggested that the flow was inherently unsteady, and that the flow at some parts of the cycle were frequency dependent. Using this same experimental apparatus, Krane et al. [54] further analyzed terms commonly neglected under the quasi-steady flow assumption. PIV data were used to estimate the relative magnitudes of the unsteady and convective acceleration terms of the unsteady Bernoulli equation for various configurations. Their analysis indicated that at some points of the cycle, the unsteady acceleration terms were non-negligible, suggesting the need for the inclusion of unsteady terms in analytical glottal flow models.

Deverge et al. [55] performed measurements in a mechanical vocal fold model using air as the working fluid. The model lengths were up-scaled by a factor of 3, with an inferior-superior dimension of 2 cm and an anterior-posterior dimension of 3 cm. Three different glottal shapes were considered: straight (uniform), rounded (half-circle), and Gaussian. A piston driven by an electric motor and eccentric wheel was used to move one vocal fold medially-laterally. A pressure sensor was mounted in the opposing stationary fold at the glottis midpoint, and another pressure sensor was mounted in the pipe upstream of the model glottis. Oscillation frequencies between 5 Hz and 35 Hz (which corresponded to 1/9th of the corresponding human frequency) were studied. Their results suggested that the influence of flow unsteadiness due to wall movement was negligible. The quasi-steady approximation was found to fail during times near vocal fold collision. They showed that a Bernoulli equation, modified with corrections for viscous effects, would provide a somewhat reasonable prediction of the wall pressure. Cisonni et al. [52] used this setup with straight and round geometries

to obtain similar pressure measurements to explore inverse quasi-steady and unsteady glottal flow models.

Detailed flow measurements using a hot-wire anemometer and flow visualization were reported by Mongeau et al. [56] using a mechanical model of the vocal folds with an upstream tube but no downstream tube. A flexible model of the vocal folds was constructed using silicone rubber and was driven medially-laterally using a motor assembly at frequencies of up to 150 Hz. The geometry of the glottis model was typical of the human vocal folds with a converging glottal wall profile. The size was the same scale as the human vocal folds. A photoelectric sensor was mounted upstream of the glottis, within the subglottic tube, to measure instantaneous area. Other flow measurements included time-averaged transglottal pressure, instantaneous pressure upstream using a microphone, and glottal jet velocity using hot-wire probes. Instantaneous velocity profiles for unsteady jets were compared with those for steady jets, and found to agree reasonably well except during phases near glottal closure. They estimated that the quasi-steady assumption was not valid during approximately one-fifth of the duty cycle.

The same mechanism used by Mongeau et al. [56] was used in several subsequent studies. Zhang et al. [57] included a downstream duct and used vocal fold models with converging, diverging, and straight orifice wall profiles. The quasi-steady approximation was verified by comparing measured and predicted radiated acoustic pressures for various flow rates and operating frequencies typical of human phonation. Zhang and Mongeau [58] employed wavelet analysis to analyze the broadband sound generated by the models' glottal jets. Good agreement was found between the quasi-steady approximation and measurements during open phases, but discrepancies were found near closed phases. It was hypothesized that this was related to the establishment of the jet turbulence. Park and Mongeau [47] used the model with converging and diverging orifice wall profiles to measure orifice discharge coefficients. Glottal jet velocity distributions were measured using a hot-wire probe traversed over the glottal jet for both steady and unsteady orifices. The corresponding orifice discharge coefficients were compared. For a Reynolds number above 3000 and frequency of 100 Hz, their results indicated good agreement with the quasi-steady ap-

proximation for 70% of the duty cycle. The approximation was poor for lower Reynolds numbers near the glottal closure times. Finally, Park and Mongeau [59] used this setup to explore the influence of a posterior gap on the models' characteristic flow and acoustics. The posterior gap was a 3.18 mm diameter hole at one anterior-posterior end of the model's orifice, thereby creating a constant flow superimposed on the unsteady flow during model oscillations. Orifice discharge coefficients based on hot-wire measurements, as well as radiated sound measurements, were used to analyze aerodynamic energy transfer and radiated broadband sound emission.

Shadle et al. [60] performed flow visualization using a dynamic model of the vocal folds, in which the folds were simulated using two rectangular "shutters". Only one shutter moved. Flow visualization was used to observe the jet formation. It was found that when the orifice between the shutters was moved slightly off-center, the jet attached to the nearest wall. When a constriction representing the ventricular folds was added in the downstream duct, however, the jet plume was axial, in spite of being off-center (presumably because of a gentler pressure recovery). Barney et al. [61] and Shadle et al. [62] reported experiments performed on a somewhat similar dynamic mechanical model of the vocal folds. Two electrodynamic linear actuators were used to move plates and simulate vocal fold motion. The streamwise length of the "glottis" (orifice thickness) was 3 mm. Upstream and downstream ducts were included. Hot-wire measurements were performed at several locations downstream of the orifice, and it was shown that the interaction of non-acoustic fluid motion (i.e., eddies or vortices) with the rigid duct exit resulted in additional sound production. The mechanical model was used to explore inverse filtering models and to explore the influence of the Rothenberg mask on acoustic and nonacoustic flow fields.

Alipour and Scherer [63] measured mean pressure and flow data in a hemilarynx mechanical model of the vocal folds. This model consisted of a rectangular, hard plastic piece measuring 7 mm inferiorly-superiorly and 25 mm anteriorly-posteriorly with latex sheets stretched over the plastic piece towards duct walls. The model was driven medially-laterally using a mechanical plunger that attached the plastic piece to a loudspeaker. The oscillation frequency was 100 Hz. Amplitudes ranged from 0 to 0.3 mm. A laser sensor was used to measure the

glottal gap. Airflow and transglottal pressure data were also acquired. The data were used to derive an empirical relationship for the dimensionless pressure coefficient as a function of other dimensionless parameters.

Hyakutake et al. [64] developed a mechanically-driven vocal fold model to study flow separation points and intraglottal pressure distributions. The vocal fold model was in the shape of a half cylinder with a radius of 10 mm placed opposite to a flat wall (i.e., in a hemilarynx configuration). The constriction was driven medially-laterally using a piezoelectric actuator with a peak-to-peak amplitude of 0.16 mm and at frequencies of up to 50 Hz. Pressure taps along the flat wall opposite to the oscillating model were used to acquire intraglottal pressure data and compare their results with a complementary computational model.

Rigau et al. [65] used a mechanical shutter to mimic the human vocal folds to evaluate a clinical method of assessing glottic closure. The mechanical shutter constituted an orifice resistor and consisted of a triangular-shaped opening in a circular plate placed within a 2 cm-diameter tube. The tube represented the subglottal and supraglottal vocal tracts, respectively, with the shutter separating the two sections. The opening angle varied from 4° to 27°, corresponding to areas ranging from 0.15 to 1.12 cm^2, at a relatively low frequency to simulate glottal opening during breathing. A loudspeaker was used to generate an acoustic signal within the supraglottal vocal tract. They reported that this method, termed the "forced oscillation technique" (FOT), could be used as a non-invasive method to assess glottic closure.

4.2 Non-uniform-phase driven models

Driven models summarized to this point have been driven with medial-lateral motion that acts uniformly over the vocal fold model. We now consider driven models in which the glottal profile – and not just the glottal width – changes. One very important quality of this type of model is that it is able to generate the alternating, convergent-divergent type of motion that is typical of human phonation.

Triep et al. [66] reported on a model based on two counter-rotating cams, each

of which was covered by a stretched silicone membrane, and each representing one vocal fold (fig. 7). The model was scaled up by a factor of 3 and operated in a water tunnel; consequently, the frequency was reduced by a factor of 135. Ventricular folds were included in the supraglottal test section in some configurations. Time-resolved PIV was used to map the flow with and without ventricular folds at different phases of the oscillation cycle. Strong asymmetric recirculation zones were observed, apparently due to phenomena similar to the Coanda effect. Highly three-dimensional flow characteristics were observed in the supraglottal jet. Triep and Brücker [67] performed further flow analysis using this model, including volume velocity waveform calculation, flow visualization using fluorescent dye injection, and velocity vector field characterization using PIV. The jet evolution was documented by acquiring data in both midcoronal and midsagittal planes. Axis-switching and other flow phenomena were observed and discussed. Triep et al. [68] introduced new cam geometries for the same setup. They used three-dimensional high-speed stereoscopic imaging from an excised human larynx model as the basis for the new geometries. Optimization techniques were used to define cam geometries that yielded four different glottal closure types of interest (convex, concave, rectangular, and triangular). Kirmse et al. [69] used different configurations of these cam geometries, including asymmetric driving functions, to explore the glottal jet in regular and pathological cases.

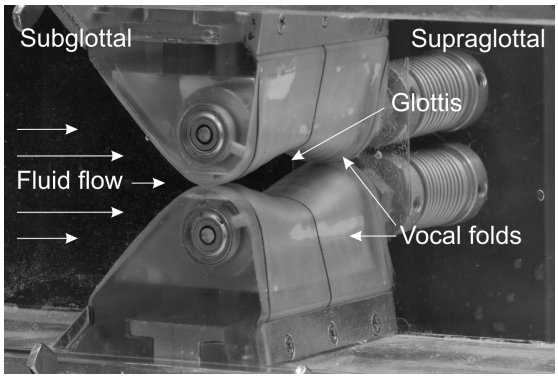

Figure 7: Test setup with externally driven vocal folds proposed by Triep et al. [66, 67, 68]

In another type of mechanically-driven vocal fold model, Kucinschi et al. [70]

described measurements in which motion was driven using two independently-controlled stepper motors. Two cylinders were placed such that they formed the glottal exit and entrance radii of one vocal fold model. Latex strips were attached at one end to the subglottic duct, wrapped over the two cylinders, and attached at the other end to the supraglottic duct, thereby forming the vocal fold surface. The two cylinders were driven laterally using two independently-controlled motor-and-lever-driven mechanisms. In this manner the cylinders could be driven either in-phase or out-of-phase. Two opposing vocal folds were fabricated in this manner. The model was scaled up from human dimensions by a factor of 7.5, giving an intraglottal inferior-superior length of approximately 2.6 cm. The glottal gap ranged from approximately 1.88 to 7.8 mm (0.25 to 1.04 mm human-size). The frequency of oscillation ranged from 0.5 to 2 Hz, corresponding to human-scale frequencies of 28.1 to 112.5 Hz. Flow rate, transglottal pressure, and flow resistance data were reported for a variety of parameter values. Flow visualization was used to compare steady and unsteady glottal jets generated by the model as it assumed identical positions. The model results were also used to generate data for comparison with computational model simulations.

5 Self-oscillating models

As discussed above, the fundamental mechanism of human phonation is vocal fold flow-induced vibration which generates the basic tone of the human voice. The periodic motion of these two elastic structures is attributed to a fluid-structure-acoustic interaction. The experimental approaches of the above-described static and driven artificial models were focused mainly on aerodynamic investigations. In several works the acoustic production was additionally analyzed [51, 50, 59]. However the complete fully-coupled fluid-structure-acoustic interaction relationships were not able to be observed because of simplifications in the experimental strategies. Therefore a large effort has been made to develop life-sized artificial vocal folds which show similar behaviour as human vocal folds during phonation. Achieving flow-induced oscillations means that the fully-coupled process can be studied in detail. For example, in addition

to aerodynamics, the total radiated acoustic field (tonal and broadband components) as well as the structural dynamics of vocal folds can be investigated. However, there have been numerous difficulties to overcome in the development of self-oscillating models, such as achieving satisfactory model and measurement repeatability using materials with very low Young's moduli, and obtaining suitable experimental access given the constraints of small spatial and temporal scales. The number of research groups using such elastic models of the vocal folds has significantly increased lately. Most groups have used geometrically and materially simplified vocal fold models. Reports in the literature in which these models have been used have focused mainly on the coupled process, e.g., the phonation threshold pressure (i.e., the minimum subglottal pressures for oscillation onset and offset), the aerodynamics, and the structural motion. Additionally, an interesting application has been the flow-structure coupling with acoustic sources as well as acoustic sound production.

The following literature review is subdivided as follows. First, models with mostly simplified geometries are discussed. Second, models with more realistic geometries and with homogeneous material distributions are presented. These are finally followed by a discussion of multi-layer models mimicking the material properties and inner structure of the human vocal folds.

5.1 Models with simplified geometry

One of the early significant works using flexible vocal fold models was that of Titze et al. [71]. They used a life-sized model in a hemilarynx configuration without supraglottal tract. The artificial vocal fold consisted of a rigid body and a silicone membrane which encapsulated a liquid representing the vocal fold mucosa. Flow-induced oscillation of the artificial mucosa was achieved for various subglottal pressures, prephonatory glottal half-widths, and artificial mucosa liquid viscosities. Adjusting these parameters they measured the phonation threshold pressure for oscillation onset and offset. Hysteresis behaviour was observed, in that the pressure was found to be lower for oscillation offset than for onset. The lowest threshold pressure was found for a gap between 0 and 0.1 mm and the lowest selected viscosity of the liquid. These results confirmed, in gen-

eral, the predictions made by the small amplitude analysis reported by Titze [16]. That analysis was based on the assumption of negligible vocal fold body motion but included the acoustic inertance of the supraglottal duct. Chan et al. [72] used the same model to explore the dependence of phonation threshold pressure on membrane thickness and glottal convergence angle. Chan and Titze [73] additionally presented results of an updated experimental setup including a supraglottal channel. Moreover the encapsulated fluid simulating the superficial layer of the lamina propria (see fig. 4) was changed to use viscoelastic biomaterials which are commonly used by surgeons for repairing defects in the lamina propria. The small amplitude analysis was adjusted to include both the mucosal wave and the supraglottal acoustic inertance as primary energy transfer mechanisms for obtaining self-sustained vocal fold vibrations. The experimental results showed that the phonation threshold pressure was significantly lowered by the influence of the supraglottal channel. This effect was consistent with the small amplitude analysis. Further experiments studied different biomaterials adapting the superficial layer which were implanted in the model using a standard surgical technique.

Kataoka et al. [74] investigated the oscillation frequency (f_0) dependence on the transglottal pressure (p), the extension length, and the model mass. The model was formed from the finger part of a surgical glove and the end forming the glottis was folded back on itself. Pre-tension was realized by stretching the lateral end of the glottal side of the model. For enhancing the mass of the vibrating portion, a paste was inserted in pockets which had been shaped by everting the glottal end of the tube. The results documented a strong influence of the parameter on the oscillation frequency f_0. In a later work Owaki et al. [75] investigated the influence of the stiffness of the vocal fold model on f_0. Stiffness was increased by injecting air in the gas-tightened pockets of the artificial vocal folds. They discussed the idea that the raising of a low f_0 in human voice is predominantly done by increasing the stiffness of the vocal folds due to the contraction of the thyroarytenoid and the cricothyroid muscles.

Another simplified model of the vocal folds was introduced by Ruty et al. [76]. They used two silicone tubes filled with water which were mounted parallel to each other in a metal frame. Air flowed through the gap between the tubes,

exciting the tubes to self-sustained oscillations. A resonance supraglottal tube with constant diameter of 2.5 cm and a varying length was integrated in the test rig. Controlling the pressure of the water in the silicone tubes, they investigated the oscillation frequency as well as the phonation threshold onset and offset pressure in subglottal region. The results were in good agreement with data obtained in human phonation. The phonation onset and offset hysteresis effect reported by Titze [71] and Chan and Titze [73] was also confirmed. The model was additionally used to validate theoretical low-order models of human phonation by incorporating the flow field, the structural dynamics, and the acoustic coupling to the vocal tract [77]. In this study two supraglottal tubes with different lengths: 250 and 500 mm, corresponding to resonance frequencies of 340 and 170 Hz, respectively, were used. Regarding the fundamental frequency and the oscillation threshold pressure, the theoretical model showed qualitatively similar results for various pressures in the model tubes. Quantitative deviations accounted for the assumptions in the simplified theoretical models, particularly the neglecting of the three-dimensional motion of the silicone tubes and of the fluid flow. A revised version of the mechanical model was applied by van Hirtum et al. [78]. Independent control of the width of the initial glottis opening and the initial pressure of the water within the silicone tubes was implemented. Furthermore it was possible to measure the dimensions of the glottal opening during the oscillations by an optical measurement technique. In their investigations they studied the influence on oscillation threshold pressure of the two independent initial parameters of oscillation frequency and glottal aperture during a cycle. It was found that the oscillation threshold pressure (onset and offset) increased for larger initial glottal width and for higher internal pressure in the model tubes. Similar behaviour was found for the oscillation frequency. Further extension of this test setup was reported by Bailly et al. [13] by including the ventricular folds in the supraglottal region. In addition to the elastic replica of the vocal folds, they also used a static replica to estimate the pressure drops across the vocal folds and the ventricular folds separately. Due to an under-pressure within the ventricular gap, they hypothesized that the ventricular folds could oscillate. Using the elastic model, the influence of the ventricular folds on the occurrence of self-sustained oscillations was studied in

detail. The results showed that the oscillations can be forced or even suppressed by the ventricular folds, depending on their aperture. Suppression was achieved for small apertures in the range of the glottal gap, or even smaller, whereas enhancement was yielded for larger distances.

Another model was developed by Deguchi et al. [79]. They threaded two silicone rubber sheets through slits in opposing walls of a rectangular channel. The shape of the slits was similar to the outer outline of the cross section of the human vocal folds. The purpose of the investigations was to analyse the dependence of oscillation onset pressure on the initial aperture of the glottis and the pre-tension in the rubber sheets. Two ends of the sheets on the same side were coupled to a force-gauge, and by stretching the sheet to a specific length, the pre-tension could be controlled. They observed a wavelike motion of the model which spread over the entire surfaces of the rubber sheets. By increasing the pre-tension and reducing the initial glottal gap, the motion was attenuated and the oscillation onset pressure was enhanced.

5.2 Models with homogeneous material distribution

Models that feature precise control over initial geometry have recently begun to be developed. Thomson et al. [80] developed a flexible model consisting of homogeneous and isotropic polyurethane rubber in a hemilaryngeal configuration. The material Young's modulus was 13.7 kPa (fig. 8). The geometry was based on the M5 model of Scherer et al. [12] and was life-sized. For a constant subglottal pressure, the artificial vocal fold vibrated at a frequency of 89 Hz. In a later work [81] they reported on a complete laryngeal setup with two artificial vocal folds that were each equal to the initial hemilarynx vocal fold. For this configuration the oscillation frequency of the artificial vocal folds was approximately 120 Hz. The model was used for validating a numerical two-dimensional finite element model. The applied numerical model captured the fully-coupled fluid-structure interaction dynamics. The results showed a greater net pressure distribution within the glottis in the period of positive energy transfer into the solid domain as in the period of negative transfer. This temporal asymmetry was evidently produced by a cyclic change of the glottal profile from convergent

to divergent shape, which is expected to be one of the key factors in achieving self-sustained vocal fold oscillations [16]. Spencer et al. [82] adjusted this model setup to enable optical access to measure structural strains of the superior surface of the artificial vocal folds. A special optical system was designed and constructed. The oscillations were recorded by a high-speed camera. Applying a correlation technique it was possible to obtain the three-dimensional displacement of the vocal fold structure. Considering the incompressibility of the material, the structural stress was calculated. Based on these data the contact pressure on the medial surface was estimated by using a Hertzian impact model introduced by Johnson [83]. The calculations showed a nonlinear dependence between the contact pressure and the flow rate.

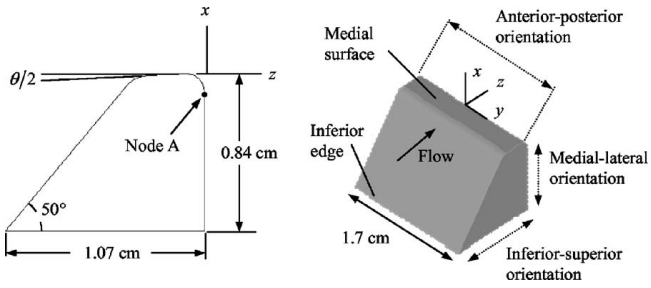

Figure 8: Flexible vocal fold model consisting of polyurethane rubber proposed by Thomson et al. [80] based on the geometry of the M5 model by Scherer et al. [12] displayed in the fig. 6

A similar phonation model in human life-size was developed by Becker et al. [19] in which they studied the full fluid-structure-acoustic coupled process. The test rig included a complete larynx configuration with a supraglottal channel extending 230 mm from the glottal exit. The artificial models consisted of a polyurethane rubber with an elastic modulus in the range of 6.5 kPa. The transient flow field was captured by a phase-resolved PIV technique within an oscillation cycle. They found that an asymmetric flow field, characterized by a jet separating from one vocal fold and attaching to the other, was formed due to the Coanda effect and to asymmetric geometrical conditions in the glottal duct. The attached side changed stochastically from cycle to cycle. The detected sound signal could be divided into tonal and broadband components. Correlations between the acoustic signal and the velocity signal measured by a hotwire

probe related the tonal components to the oscillating flow rate. Moreover, the broadband noise was found to not be associated with the vortex structures in the shear layers of the jet, but was suggested to be the result of vortices which interacted with the superior surfaces of the artificial vocal folds, similar to trailing edge noise [84].

In the study by Šidlof et al. [85], the supraglottal flow field was observed using a 4:1 scaled physical model of the vocal folds. The model was cast using an RTV-II type 69199 two-compound silicone rubber. The upper vocal fold was fixed in the channel, whereas the second vocal fold was mounted on four flat springs set into the wall of the channel. The prephonatory abduction of the vocal folds was set by two adjusting screws. The channel was extended downstream of the vocal fold models by a device accounting for the supraglottal region. Detailed high-resolution, phase-resolved PIV measurements of the supraglottal regions were performed with varying flow rate. The flow field was characterized by a jet penetrating in the supraglottal region skewed to either the top or the bottom of the channel. This phenomena, as well as the temporal evolution of the velocity field, is very similar to the findings of Becker et al. [19]. In a newer study Šidlof et al. [86] investigated the separation point of the glottal jet from the vocal fold models during an oscillation cycle within a similar test setup using phase-resolved PIV. Shortly proir or after the total glottal closure the separation occured much more downstream as it was considered in simplified flow models based on Bernoulli or Euler equations. In a another work, Horáček et al. [15] applied time-resolved PIV to measure the velocity distribution in the glottal region of complex physical models of the voice production. The material of their human life-size model was composed of polyurethane rubber. The test setup included a trachea and a human vocal tract with acoustical spaces obtained by magnetic resonance images (MRI). Simultaneously with PIV measurements, the subglottal pressure, the radiated acoustic pressure, and the vibration of the vocal folds were recorded within a physiological range of mean airflow rate and fundamental phonation frequency of 158 Hz. Images of the vibrating vocal folds were captured by a high-speed camera. The flow field showed large vortex structures in a wider region above the ventricular folds, the laryngeal cavity, and epilarynx tube. Their dimensions were comparable with the channel cross-

section. These vortices disappeared in the narrower pharyngeal part of the vocal tract model where the flow became more uniform. The experiments were also used for validating a numerical finite element model with prescribed vocal fold motion [87].

A detailed analysis of the flow field beyond the vocal folds was also performed by Neubauer et al. [28]. They measured the supraglottal flow distribution with PIV at different time points within an oscillation cycle. As test device, the artificial vocal folds developed by Thomson et al. [81] were used in a complete larynx configuration, including a supraglottal extension. Applying a spatio-temporal analysis based on the method of empirical orthogonal eigenfunctions on the PIV data, they separated different flow structures to characterize vortex generation, vortex convection, and jet flapping. Vortex generation was observed in the free shear layers of the jet and these vortices were convected downstream. Jet flapping occurred during one cycle, i.e., the jet oscillated around a middle position with small amplitude. This phenomenon was related to an antisymmetric large-scale vortex array moving downstream. Furthermore the jet yielded an asymmetrical structure with respect to the centerline in the supraglottal region due to the Coanda effect. The same analyzing technique was used by Berry et al. [88]. They investigated irregular vocal fold oscillations in a hemilarynx configuration. The vocal fold was based on the M5 model by Scherer et al. [12] and consisted of silicone rubber with a Young's modulus of about 3 kPa. For studying the structural oscillations the medial surface was imaged by a high-speed camera through a glass prism. From these images the three-dimensional movement was quantified. Additionally, the subglottal acoustic pressure and the mean subglottal pressure signals were measured. The spatiotemporal analysis yielded the dynamic eigenfunctions of the medial surface motion. It was found that strong low-ordered eigenfunctions were entrained with each other, whereas weaker high-ordered eigenfunctions were influenced and triggered by subglottal resonances. Hence, irregular vibrations for the subharmonic phonation and biphonation could be identified.

All of the above-described studies concerning oscillating vocal fold models concentrated mostly on the structural dynamics of the vocal folds, the fluid flow in the subglottal region, and the acoustic signal spread to the far field. However,

nonlinear phenomena within the phonation process, such as various oscillation onset types, register changes, and frequency jumps were not thoroughly explored, but were attributed to the biomechanical properties of the vocal fold tissue. Zhang et al. [89] investigated the acoustic coupling of the subglottal volume to dynamics of a self-oscillating vocal fold model. Measuring the oscillation onset and offset pressure threshold, as well the oscillation frequency for different lengths of a subglottal tube, they found the acoustic resonances to have a strong influence on the vocal fold model dynamics. The oscillation frequency jumped with increasing subglottal tube lengths from the first, over the second, and up to the fourth resonance frequencies. Furthermore they demonstrated different types of oscillation onset, also depending on the subglottal tube length. It is concluded that such a coupling also happens between a supraglottal tract and the laryngeal dynamics. Thus the authors advised that a detailed analysis of acoustic resonances should be done during development of an experimental setup for flexible vocal fold models. In a subsequent paper by Zhang et al. [27], they studied the difference between aerodynamically- and acoustically-driven vibrations of the vocal fold models. They used a hemilarynx model based on the M5 geometry, with vocal folds consisting of silicone rubber with a Young's modulus of approximately 11 kPa. In accordance with the investigations by Berry et al. [88] they captured the medial surface of the vocal fold through a glass prism using a high-speed camera. A spatiotemporal analysis was used to calculate the eigenmodes of the medial surface dynamics. Varying the subglottal tube length, they identified a so-called x-10 eigenmode of the medial surface dynamics for acoustically-driven vibration at the frequency of the subglottal resonance, whereas aerodynamically-driven vibrations were described by two strong eigenmodes x-11 and x-10. However in this case the model did not vibrate naturally. When the superior surface motion of the model was constrained, it oscillated at a frequency which was independent of the acoustic resonances of the subglottal region. In a later study [90] they investigated the influence of the Young's modulus reducing it from about 11 kPa down to 3 kPa. In the experiments a complete larynx as well as a hemilarynx configuration was used. The results showed that for decreasing stiffness, aerodynamically-driven vibrations occurred even for short, clinically relevant tracheal tubes. In this case a near-

field fluid-structure interaction coupling was explained to have governed the driving process. For long tracheal tubes acoustic-structure interactions led to oscillations in the range of the resonance frequency of either the subglottal or the supraglottal tube. The dynamic patterns exhibited strong inferior-superior oscillations of the vocal folds. The phonation threshold pressure was significantly reduced compared to the case of aerodynamically driven vibrations. In a recent work Zhang et al. [91] they studied the vibratory behaviour of an asymmetric vocal fold model in complete-larynx configuration compared to that of each individual vocal fold in a hemilaryngeal configuration. The models were similar to those used in [90]. One model had an isotropic material distribtion consisting of polyurethane rubber. The second possess a rigid body covered by a soft rubber layer with the same material properties of the single-layer model. They found a fundamental frequency ratio between both models in hemi-configuration of 1:3. In complete configuration the vibratory behaviour was dominated by one vocal fold constraining the other to vibrate at the same frequency. The dominance depended strongly on the subglottal pressure leading to changes in both vibratory states.

5.3 Multi-layer models

Considering the multi-layer structure of the human vocal folds, Drechsel and Thomson [92] developed a two-layer model with gross geometry based again on the M5 model of Scherer et al. [12]. It consisted of a 2 mm silicone cover-layer with a Young's modulus of 4.1 kPa and a body also made of silicone with a modulus of 22.5 kPa. The subglottal tube had a length of 60 cm for minimizing the subglottal oscillation onset pressure. Three different supraglottal configurations were studied: an open-jet case, a vocal tract case, and a ventricular folds case. In the latter case two rigid ventricular folds were inserted in the vocal tract tube. For the configurations with vocal tract, the position of the supraglottal tube was varied in the direction orthogonal to the glottal slit (i.e., in the medial-lateral direction). Phase-resolved PIV was used to investigate the supraglottal flow field. In all supraglottal configurations a starting vortex could be detected which shed downstream. Including the ventricular folds caused this shedding

to be partially obstructed. Furthermore, in the vocal tract cases, the jet was skewed to the nearest wall of the supraglottal tube in the case of asymmetric vocal tract position. In contrast to this it was skewed away from the nearest wall in the presence of the ventricular folds. Calculations of jet fluctuations showed that the lowest level of fluctuation was obtained for an open jet. In contrast, in the vocal tract cases yielded the highest jet fluctuations, suggesting a stabilizing influence of the ventricular folds on the arising jet.

This two-layer vocal fold model concept was also used by Riede et al. [32] in a study of non-human mammalian vocalization and by Pickup and Thomson [30] to study asymmetric vocal fold motion. In the latter study, they varied the stiffness of the cover and the body of one fold to create a model in which the two opposing vocal folds were of different stiffness. Using an open jet condition without a vocal tract model, the structural dynamics, the supraglottal flow field, and the oscillation onset pressure were analysed. For asymmetric material properties of the vocal folds, the results showed reduced glottal width and a significant phase shift in the vibrations between the two vocal folds. Furthermore, the oscillation onset pressure and the skewness of the glottal jet were increased, compared to the folds with symmetric material properties. It was supposed that this could potentially contribute to broadband sound generation.

To overcome some unrealistic aspects of some of the aforementioned artificial vocal fold models, Pickup and Thomson [26] developed a two-layer vocal fold model with geometry derived from MRI data sets. They compared the oscillation pattern of the MRI-based models with the simplified M5 models used in [30]. Both models were fabricated with equal material properties. Recording the models from anterior and superior view by a high-speed camera, the MRI-based models showed some useful improvements in the oscillation patterns. The vertical motion was reduced, exhibiting more alternating convergent-divergent surface profiles of the glottal duct. Moreover a mucosal wave-like motion could be detected. However, the oscillation onset pressure was increased and irregularities arose in the oscillation patterns for higher subglottal pressures compared to the simplified model. They concluded that further improvements in artificial vocal fold models were still needed in order to create models that vibrate with more life-like motion.

6 Concluding remarks

Static larynx modeling has a long history and has produced much useful data about translaryngeal pressure drop and recovery, intraglottal pressure and flow profiles, flow separation points, and the characteristics of the supraglottal jet. With the advent of dynamic vocal fold modeling [60] one might be tempted to suppose that static models are no longer useful. It must be recognized, however, that all models include, by definition, simplifying assumptions and are thus applicable primarily within the context of the experimental questions they were designed to answer. Static models can still offer much relevant information regarding the specifics of velocity and pressure profiles in a given channel geometry. They also can be a reliable tool for benchmarking theoretical and computational models of glottal flow.

The next generation vocal fold models are dynamic models. Driven vocal fold models have been fabricated that reproduce the gross motion of the vocal folds. These have been classified into uniform-phase and non-uniform-phase driven models. The former emulate the medial-lateral vibration of the folds, whereas the latter also include the convergent and divergent glottal shape change. In these dynamic models the flow is studied in a controllable environment with high repeatability, since typical motions of the vocal folds in human phonation can be repeatedly prescribed. Information regarding the intra-cycle and inter-cyclic flow structures can be extracted with good precision.

Further dynamic models are based on self-sustained oscillations of vocal fold replica made of elastic materials. The movement of the folds is due to a process similar to that of human phonation, in which the motion arises as a result of flow-structure-acoustic interactions and in which energy is exchanged between fluid and material. Besides identifying the proper geometry and material, a significant challenge in these experiments lies in the experimental setup required for measurements in life-size models with small length and short time scales of the flow and structure dynamics. Having reproduced the dynamic processes and the acoustic production it is possible to investigate the fully-coupled process of the fluid-structure-acoustic interaction. The models developed until now show a

behavior with good consistency to that of human vocal folds. However involving acoustic coupling has significantly increased the complexity of the experimental setup. Thus a systematic strategy for the test devices needs to be developed for achieving controlled basic conditions. Looking ahead it is anticipated that future work will result in the development of more advanced self-oscillating models that feature improved, more life-like motion.

Acknowledgement

Financial support from the German Research Foundation (DFG) grant no. FOR 894/1 "Strömungsphysikalische Grundlagen der Menschlichen Stimmgebung" and from the Graduate School of Advanced Optical Technologies of the University Erlangen-Nuremberg (SAOT) are gratefully acknowledged. Support for SLT from Awards R01DC009616 and R01DC005788 from the U.S. National Institute on Deafness and Other Communication Disorders (NIDCD) is gratefully acknowledged; the content is solely the responsibility of the authors and does not necessarily represent the official views of the NIDCD or the National Institutes of Health.

Disclosure Statement

The authors are not aware of any biases that might be perceived as affecting the objectivity of this review.

References

[1] Titze IR. Principles of voice production. Prentice Hall; 1994.

[2] Titze IR, Alipour F. The myoelastic aerodynamic theory of phonation. National Center for Voice and Speech; 2006.

[3] Fant G. Acoustic Theory of Speech Production. de Gruyter Mouton; 1970.

[4] Fant G. The source filter concept in voice production. STL-QPSR. 1981;22(1):21–37.

[5] McCoy S. Your Voice: An Inside View. Inside View Press; 2004.

[6] Gray H. Henry Gray's Anatomy of the Human Body; 1918.

[7] Eysholdt U, Rosanowski F, Hoppe U. Vocal fold vibration irregularities caused by different types of laryngeal asymmetry. Eur Arch Otorhinolaryngol. 2003 April;260:412–417.

[8] Kitzing P. Clinical Applications of Electroglottography. J Voice. 1990;4(3):238–249.

[9] Wendler J. Stroboscopy. J Voice. 1992;6(2):149–154.

[10] Döllinger M. The Next Step in Voice Assessment: High-Speed Digital Endoscopy and Objective Evaluation. Cur Bioinf. 2009;4:101–111.

[11] van den Berg J, Zantema JT, Doornenbal P. On the Air Resistance and the Bernoulli Effect of the Human Larynx. J Acoust Soc Am. 1957 May;29(5):626–631.

[12] Scherer RC, Shinwari D, Witt KJD, Zhang C, Kucinschi BR, Afjeh AA. Intraglottal pressure profiles for a symmetric and oblique glottis with a divergence angle of 10 degrees. J Acoust Soc Am. 2001 April;109(4):1616–1630.

[13] Bailly L, Pelorson X, Henrich N, Ruty N. Influence of a constriction in the near field of the vocal folds: physical modeling and experimental validation. J Acoust Soc Am. 2008 Nov;124(5):3296–3308.

[14] Bailly L, Henrich N, Pelorson X. Vocal fold and ventricular fold vibration in period-doubling phonation: Physiological description and aerodynamic modeling. J Acoust Soc Am. 2010 May;127(5):3212–3222. Uses same model as Ruty2007.

[15] Horáček J, Šidlof P, Uruba V, Veselý J, Radolf V, Bula V. PIV Measurement of Flow-Patterns in a Human Vocal Tract Model. In: Boone M, editor. Proceedings NAG/DAGA 2009. Rotterdam. NAG and DEGA; 2009. p. 1737–1740.

[16] Titze IR. The physics of small-amplitude oscillation of the vocal folds. J Acoust Soc Am. 1988 April;83(4):1536–1552.

[17] Titze IR. Nonlinear source-filter coupling in phonation: Theory. J Acoust Soc Am. 2008 May;123(5):2733–2749.

[18] Titze IR, Worley AS. Modeling source-filter interaction in belting and high-pitched operatic male singing. J Acoust Soc Am. 2009 September;126(3):1530–1540.

[19] Becker S, Kniesburges S, Müller S, Delgado A, Link G, Kaltenbacher M, et al. Flow-structure-acoustic interaction in a human voice model. J Acoust Soc Am. 2009 March;125(3):1351–1361.

[20] Thomson S. Fluid-Structure Interactions within the Human Larynx [Phd]. Purdue University; 2004.

[21] Min YB, Titze IR, Alipour-Haghighi F. Stress-strain response of the human vocal ligament. Ann Otol Rhinol Laryngol. 1995;104:563–569.

[22] Tran QT, Berke GS, Gerratt BR, Kreiman J. Measurement of Young's modulus in the in vivo human vocal folds. Ann Otol Rhinol Laryngol. 1993;102:584–591.

[23] Chan RW, Rodriguez ML. A simple-shear rheometer for linear viscoelastic characterization of vocal fold tissues at phonatory frequencies. J Acoust Soc Am. 2008;124(2):1207–1219.

[24] Wegel RL. Theory of Vibration of the Larynx (A). J Acoust Soc Am. 1929 October;1(1):1–21.

[25] Scherer RC, Witt KJD, Kucinschi BR. The effect of exit radii on intraglottal pressure distributions in the convergent glottis. J Acoust Soc Am. 2001 November;110(5):2267–2269.

[26] Pickup BA, Thomson SL. Flow-induced vibratory response of idealized versus magnetic resonance imaging-based synthetic vocal fold models. J Acoust Soc Am. 2010 September;128(3):EL124–EL129.

[27] Zhang Z, Neubauer J, Berry DA. Aerodynamically and acoustically driven modes of vibration in a physical model of the vocal folds. J Acoust Soc Am. 2006 Nov;120(5 Pt 1):2841–2849.

[28] Neubauer J, Zhang Z, Miraghaie R, Berry DA. Coherent structures of the near field flow in a self-oscillating physical model of the vocal folds. J Acoust Soc Am. 2007 Feb;121(2):1102–1118.

[29] Popolo PS, Titze IR. Qualification of a quantitative laryngeal imaging system using videostroboscopy and videokymography. Ann Otol Rhinol Laryngol. 2008 June;117(6):404–412.

[30] Pickup BA, Thomson SL. Influence of asymmetric stiffness on the structural and aerodynamic response of synthetic vocal fold models. J Biomech. 2009 Oct;42(14):2219–2225.

[31] Zhang Z. Characteristics of phonation onset in a two-layer vocal fold model. J Acoust Soc Am. 2009 February;125(2):1091–1102.

[32] Riede T, Tokuda IT, Munger JB, Thomson SL. Mammalian laryngeal air sacs add variability to the vocal tract impedance: Physical and computational modeling. J Acoust Soc Am. 2008 July;124(1):634–647.

[33] Ishizaka K, Matsudaira M. Fluid Mechanical Considerations of Vocal Cord Vibration. Speech Communication Research Lab, Santa Barbara, CA. 1972;Monograph 8.

[34] Scherer RC, Titze IR, Curtis JF. Pressure-flow relationships in two models of the larynx having rectangular glottal shapes. J Acoust Soc Am. 1983 Feb;73(2):668–676.

[35] Fulcher LP, Scherer RC, Zhai G, Zhu Z. Analytic representation of volume flow as a function of geometry and pressure in a static physical model of the glottis. J Voice. 2006 Dec;20(4):489–512.

[36] Binh N, Gauffin J. Aerodynamic measurements in an enlarged static laryngeal model. STL-QPSR. 1983;24(2-3):1.

[37] Li S, Scherer RC, Wan M, Wang S, Wu H. The effect of glottal angle on intraglottal pressure. J Acoust Soc Am. 2006 January;119(1):539–548.

[38] Scherer RC, Torkaman S, Kucinschi BR, Afjeh AA. Intraglottal pressures in a three-dimensional model with a non-rectangular glottal shape. J Acoust Soc Am. 2010 August;128(2):828–838.

[39] Alipour F, Scherer RC. Pressure and velocity profiles in a static mechanical hemilarynx model. J Acoust Soc Am. 2002 Dec;112(6):2996–3003.

[40] Fulcher LP, Scherer RC, Witt KJD, Thapa P, Bo Y, Kucinschi BR. Pressure distributions in a static physical model of the hemilarynx: measurements and computations. J Voice. 2010 Jan;24(1):2–20.

[41] Coanda H. Device for deflecting a stream of elastic fluid projected into an elastic fluid. US Patent 2052869;1935 April.

[42] Pelorson X, Hirschberg A, van Hassel RR, Wijnands APJ, Auregan Y. Theoretical and experimental study of quasisteady-flow separation within the glottis during phonation. Application to a modified two-mass model. J Acoust Soc Am. 1994 Dec;96(6):3416–3431.

[43] Shinwari D, Scherer RC, DeWitt KJ, Afjeh AA. Flow visualization and pressure distributions in a model of the glottis with a symmetric and oblique divergent angle of 10 degrees. J Acoust Soc Am. 2003 January;113(1):487–497.

[44] Scherer RC, Shinwari D, Witt KJD, Zhang C, Kucinschi BR, Afjeh AA. Intraglottal pressure distributions for a symmetric and oblique glottis with a uniform duct (L). J Acoust Soc Am. 2002 October;112(4):1253–1256.

[45] Hofmans GCJ, Groot G, Ranucci M, Graziani G, Hirschberg A. Unsteady flow through in-vitro models of the glottis. J Acoust Soc Am. 2003 March;113(3):1658–1675.

[46] Erath BD, Plesniak MW. An investigation of bimodal jet trajectory in flow through scaled models of the human vocal tract. Exp Fluids. 2006 February;40(5):683–696.

[47] Park JB, Mongeau L. Instantaneous orifice discharge coefficient of a physical, driven model of the human larynx. J Acoust Soc Am. 2007 Jan;121(1):442–455.

[48] Li S, Wan M, Wang S. The effects of the false vocal fold gaps on intralaryngeal pressure distributions and their effects on phonation. Sci China C Life Sci. 2008 Nov;51(11):1045–1051.

[49] Alipour F, Scherer RC, Knowles J. Velocity Distributions in Glottal Models. J Voice. 1996;10(1):50–58.

[50] Kucinschi BR, Scherer RC, DeWitt KJ, Ng TTM. Flow visualization and acoustic consequences of the air moving through a static model of the human larynx. J Biomech Eng. 2006 Jun;128(3):380–390.

[51] Zhang Z, Mongeau L, Frankel SH, Thomson S, Park JB. Sound generation by steady flow through glottis-shaped orifices. J Acoust Soc Am. 2004 September;116(3):1720–1728.

[52] Cisonni J, Hirtum AV, Pelorson X, Willems J. Theoretical simulation and experimental validation of inverse quasi-one-dimensional steady and unsteady glottal flow models. J Acoust Soc Am. 2008 Jul;124(1):535–545.

[53] Krane M, Barry M, Wei T. Unsteady behavior of flow in a scaled-up vocal folds model. J Acoust Soc Am. 2007 December;122(6):3659–3670.

[54] Krane MH, Barry M, Wei T. Dynamics of temporal variations in phonatory flow. J Acoust Soc Am. 2010 July;128(1):372–383.

[55] Deverge M, Pelorson X, Vilain C, Lagree PY. Influence of collision on the flow through in-vitro rigid models of the vocal folds. J Acoust Soc Am. 2003 December;114(6):3354–3362.

[56] Mongeau L, Franchek N, Coker CH, Kubli RA. Characteristics of a pulsating jet through a small modulated orifice, with application to voice production. J Acoust Soc Am. 1997 August;102(2):1121–1133.

[57] Zhang Z, Mongeau L, Frankel SH. Experimental verification of the quasi-steady approximation for aerodynamic sound generation by pulsating jets in tubes. J Acoust Soc Am. 2002 October;112(4):1652–1663.

[58] Zhang Z, Mongeau LG. Broadband sound generation by confined pulsating jets in a mechanical model of the human larynx. J Acoust Soc Am. 2006 June;119(6):3995–4005.

[59] Park JB, Mongeau L. Experimental investigation of the influence of a posterior gap on glottal flow and sound. J Acoust Soc Am. 2008 August;124(2):1171–1179.

[60] Shadle CH, Barney AM, Thomas DW. An investigation into the acoustics and aerodynamics of the larynx. In: Gauffin, Hammarberg B, editors. Vocal Fold Physiology: Acoustic, Perceptual and Physiological Aspects of Voice Mechanisms. Singular Publishing Group; 1991. p. 73–82.

[61] Barney A, Shadle CH, Davies POAL. Fluid flow in a dynamic mechanical model of the vocal folds and tract. I. Measurements and theory. J Acoust Soc Am. 1999 January;105(1):444–455.

[62] Shadle CH, Barney A, Davies POAL. Fluid flow in a dynamic mechanical model of the vocal folds and tract. II. Implications for speech production studies. J Acoust Soc Am. 1999 January;105(1):456–466.

[63] Alipour F, Scherer RC. Effects of oscillation of a mechanical hemilarynx model on mean transglottal pressures and flows. J Acoust Soc Am. 2001 September;110(3):1562–1569.

[64] Hyakutake T, Deguchi S, Shiota A, Nishioka Y, Yanase S, Washio S. Effect of Constriction Oscillation on Flow for Potential Application to Vocal Fold Mechanics: Numerical Analysis and Experiment. J Biomech Sci Eng. 2006 June;1(2):290–303.

[65] Rigau J, Farre R, Trepat X, Shusterman D, Navajas D. Oscillometric assessment of airway obstruction in a mechanical model of vocal cord dysfunction. J Biomech. 2004 Jan;37(1):37–43.

[66] Triep M, Brücker C, Schröder W. High-speed PIV measurements of the flow downstream of a dynamic mechanical model of the human vocal folds. Exp Fluids. 2005 July;39(2):232–245.

[67] Triep M, Brücker C. Three-dimensional nature of the glottal jet. J Acoust Soc Am. 2010 Mar;127(3):1537–1547.

[68] Triep M, Brücker C, Stingl M, Döllinger M. Optimized transformation of the glottal motion into a mechanical model. Medical Engineering & Physics. 2010 November;in press.

[69] Kirmse C, Triep M, Brücker C, Döllinger M, Stingl M. Experimental flow study of modeled regular and irregular glottal closure types. Logopedics Phoniatrics Vocology. 2010 April;35(1):45–50.

[70] Kucinschi BR, Scherer RC, DeWitt KJ, Ng TTM. An experimental analysis of the pressures and flows within a driven mechanical model of phonation. J Acoust Soc Am. 2006 May;119(5):3011–3021.

[71] Titze IR, Schmidt SS, Titze MR. Phonation threshold pressure in a physical model of the vocal fold mucosa. J Acoust Soc Am. 1995 May;97(5):3080–3084.

[72] Chan RW, Titze IR, Titze MR. Further studies of phonation threshold pressure in a physical model of the vocal fold mucosa. J Acoust Soc Am. 1997 June;101(6):3722–3727.

[73] Chan RW, Titze IR. Dependence of phonation threshold pressure on vocal tract acoustics and vocal fold tissue mechanics. J Acoust Soc Am. 2006 April;119(4):2351–2362.

[74] Kataoka H, Kitajima K, Owaki S. Effects of transglottal pressure on fundamental frequency of phonation: study with a rubber model. Ann Otol Rhinol Laryngol. 2001 Jan;110(1):56–62.

[75] Owaki S, Kataoka H, Shimizu T. Relationship between transglottal pressure and fundamental frequency of phonation–study using a rubber model. J Voice. 2010 Mar;24(2):127–132.

[76] Ruty N, Hirtum AV, Pelorson X, Lopez I, Hirschberg A. A mechanical experimental setup to simulate vocal folds vibrations. Preliminary results. ZAS Papers in Linguistics. 2005;40:161–175.

[77] Ruty N, Pelorson X, Hirtum AV, Lopez-Arteaga I, Hirschberg A. An in vitro setup to test the relevance and the accuracy of low-order vocal folds models. J Acoust Soc Am. 2007 January;121(1):479–490.

[78] van Hirtum A, Cisonni J, Ruty N, Pelorson X, Lopez I, van Uittert F. Experimental Validation of Some Issues in Lip and Vocal Fold Physical Models. Acta Acustica. 2007 March/April;93(2):314–323.

[79] Deguchi S, Miyake Y, Tamura Y, Washio S. Wavelike Motion of a Mechanical Vocal Fold Model at the Onset of Self-Excited Oscillation. J Biomech Sci Eng. 2006 July;1(1):246–255.

[80] Thomson SL, Mongeau L, Frankel FH. Physical and numerical flow-excited vocal fold model. In: Third International Workshop MAVEBA; 2003. .

[81] Thomson SL, Mongeau L, Frankel SH. Aerodynamic transfer of energy to the vocal folds. J Acoust Soc Am. 2005 September;118(3):1689–1700.

[82] Spencer M, Siegmund T, Mongeau L. Determination of superior surface strains and stresses, and vocal fold contact pressure in a synthetic larynx model using digital image correlation. J Acoust Soc Am. 2008 Feb;123(2):1089–1103.

[83] Johnson KL. Contact Mechanics. Reprint ed. Cambridge University Press; 1987.

[84] Blake WK. Mechanics of Flow-Induced Sound and Vibration. vol. 1 and 2. Academic; 1986.

[85] Šidlof P, Doaré O, Cadot O, Chaigne A, Horáček J. Mathematical and physical modeling of flow-induced vibrations of human vocal folds. In: International Conference on Flow Induced Vibration - FIV 2008. Prague, Czech Republic; 2008. p. 141–146.

[86] Šidlof P, Doaré O, Cadot O, Chaigne A. Measurement of flow separation in a human vocal folds model, Exp Fluids. Exp Fluids. 2011;in press.

[87] Horáček J, Gráf S. Mathematical modelling of airflow in the glottal region and its comparison with experimental data. In: Proceedings 6th International Workshop on Models and Analysis of Vocal Emissions for Biomedical Applications – MAVEBA 2009. Firenze, Italy: Firenze University Press; 2009. p. 203–206.

[88] Berry DA, Zhang Z, Neubauer J. Mechanisms of irregular vibration in a physical model of the vocal folds. J Acoust Soc Am. 2006 Sep;120(3):EL36–EL42.

[89] Zhang Z, Neubauer J, Berry DA. The influence of subglottal acoustics on laboratory models of phonation. J Acoust Soc Am. 2006 Sep;120(3):1558–1569.

[90] Zhang Z, Neubauer J, Berry DA. Influence of vocal fold stiffness and acoustic loading on flow-induced vibration of a single-layer vocal fold model. J Sound Vib. 2009;322(1-2):299–313.

[91] Zhang Z. Vibration in a self-oscillating vocal fold model with left-right asymmetry in body-layer stiffness. J Acoust Soc Am. 2010 November;128(5):279–285.

[92] Drechsel JS, Thomson SL. Influence of supraglottal structures on the glottal jet exiting a two-layer synthetic, self-oscillating vocal fold model. J Acoust Soc Am. 2008 Jun;123(6):4434–4445.